X-ray interference in ultrathin epitaxial layers: A versatile method for the structural analysis of single quantum wells and heterointerfaces

L. Tapfer and K. Ploog
Max-Planck-Institut für Festkörperforschung, Heisenbergstrasse 1, D-7000 Stuttgart 80, Federal Republic of Germany
(Received 1 May 1989)

We report a versatile method to investigate the structural properties of ultrathin-epitaxial-layer structures by using the x-ray interference effect (Pendellösung). A detailed theoretical and experimental study on $Al_xGa_{1-x}As/GaAs$ heterostructures shows that the intensity modulation of the interference fringes can be used to determine the thickness, the lattice strain, and the chemical composition of single-quantum-well structures as well as of laser and high-electron-mobility-transistor structures, and the strain at heterointerfaces. We show that epitaxial layers and transition regions at heterointerfaces having a thickness of one monolayer only can be detected experimentally and analyzed by using the dynamical x-ray diffraction theory.

I. INTRODUCTION

Single-quantum-well heterostructures and thin epitaxial layers comprised of III-V semiconductors are of great interest due to their unique optical and electronic properties and their implications for the development of heterostructure devices. For a full understanding of the optical and electronic properties, it is of fundamental importance to have an accurate knowledge of the structural parameters, such as epilayer thickness, lattice strain, and chemical composition.

X-ray diffraction methods, especially the double-crystal x-ray diffraction technique, are now widely used for the structural investigation of multilayered semiconductor heterostructures. The experimental diffraction patterns obtained from multiple-quantum-well heterostructures, superlattices, and thick epitaxial layers (layer thickness >100 nm) have been analyzed and studied extensively by using kinematic,[1] semikinematic,[2] and dynamical diffraction theories.[3–5] With decreasing layer thickness, however, it becomes very difficult to investigate the structural properties of epitaxial layers in detail. Several methods have been proposed and applied to overcome these difficulties, such as extremely asymmetrical diffraction geometries,[6,7] grazing-incident diffraction,[8–10] triple-crystal diffractometry,[11] and the x-ray truncation-rod technique.[12,13] The standing x-ray wave-field technique was used to study thin epitaxial $CoSi_2$ films and the heterointerface between silicon and the silicide layer.[14,15] However, these methods are limited to structures beneath the crystal surface.

In this work we show that the x-ray interference effect (Pendellösung)[16] provides a very powerful tool to investigate quantitatively very-thin single-quantum-well structures and ultrathin epilayers made of the AlAs/GaAs system. The Pendellösung effect was predicted by the dynamical diffraction theory and it was observed in the transmission[17] and reflection mode of thin crystal slabs.[18] We show that the Pendellösung fringes, which are frequently used to determine the epilayer thickness in the range between 100 and 1000 nm, are modulated in intensity,[19,20] if a thin layer is separating two or more crystal slabs.

The experimental technique and the sample configurations are briefly described in Sec. II. The basic concepts of the interference of x-ray wave fields between epitaxial layers using a kinematical approach are given in Sec. III. The theoretical and experimental results are then presented and discussed in Sec. IV.

II. EXPERIMENTAL

The experiments were carried out using a high-resolution computer-controlled double-crystal x-ray diffractometer,[2] and utilizing a conventional 1.5-kW generator with a copper target ($\lambda_{\mathrm{Cu}\,K\alpha_1}=0.1540562$ nm). A well-collimated monochromatic x-ray beam was obtained by using an asymmetric (100) Ge crystal and the (400) reflection. The angular divergence of the x-ray beam incident on the sample was calculated to be 11 μrad. This value is much smaller than the intrinsic full width at half maximum of the (400) GaAs peak ($=40$ μrad) and thus allows us to measure the intrinsic properties of the diffraction pattern. The x-ray diffraction patterns are recorded in the vicinity of the symmetric (400) GaAs reflection. Some samples are also measured in the asymmetric diffraction geometry using the (422) reflection, where the angle of incidence is smaller than the angle between the reflected beam and the crystal surface.

The investigated samples are $Al_xGa_{1-x}As/GaAs$ heterostructures of different layer sequence grown by molecular-beam epitaxy (MBE) on [100] oriented GaAs wafers. The configurations of the samples are as follows:

(i) Type *A*: a thin GaAs layer is sandwiched between confining $Al_xGa_{1-x}As$ layers (single-quantum-well and laser structure).

(ii) Type *B*: a thin $Al_xGa_{1-x}As$ layer is capped with a relatively thick (>100 nm) GaAs layer.

III. X-RAY INTERFERENCE IN MULTILAYERED HETEROSTRUCTURES

In the dynamical diffraction theory the Pendellösung refers to the beating inside a crystal of two wave fields which are coherently related.[18] In the reflection case (Bragg case) the beating occurs between wave points on the same branch of the dispersion surface whose wave vectors are coherently related by Bloch wave criteria. If two or more layers with different lattice parameters are brought together, the wave fields of the single layers will also interfere and produce a modulation of the Pendellosung fringes. The interference of wave fields in the framework of the dynamical theory is rather complicated. In order to find out which scattering and structural parameters are critical for the interference phenomena, we first discuss the x-ray diffraction by using the kinematical approach of the dynamical theory without losing any important information. The kinematical approximation allows us to use analytical expressions which simplify the computations considerably and is still allowed if the thicknesses of the heterostructures under investigation are thinner than the x-ray extinction length.[2]

According to the kinematical theory, the reflectivity of a thin crystal plate as a function of the angular deviation ω from the Bragg angle θ_B is given by the equation

$$R=|\Phi|^2=[Y^{-1}\sin(AY)]^2 , \tag{1}$$

with

$$A=\pi\chi_h\Delta[\lambda(|\gamma_0\gamma_h|)^{1/2}]^{-1} \tag{2}$$

and

$$Y=-(|\gamma_0\gamma_h|)^{1/2}\sin(2\theta_B)\omega/\chi_h . \tag{3}$$

χ_h is the hth Fourier coefficient of the polarizability, λ the x-ray wavelength, Δ is the thickness of the layer, θ_B the kinematic Bragg angle, ω the angular deviation from the exact Bragg angle, and γ_0 and γ_h are the direction cosines of the incident and diffracted waves, respectively.

Equation (1) is valid as long as the crystal plate is thin, i.e., $A\ll 1$, which means that the layer thickness Δ is smaller than the x-ray extinction length. Due to the sinusoidal term in Eq. (1) the diffraction pattern will exhibit interference fringes.[21] The reflectivity oscillates with the period $AY=\pi$ and the distance between two fringe maxima (Pendellösung) is

$$\Delta\omega=|\gamma_h|\lambda[\sin(2\theta_B)]\Delta , \tag{4}$$

and the maximum reflectivity of the interference fringes of order n is

$$R_n(\max)=[A/(n\pi)]^2 . \tag{5}$$

Equation (5) shows that the fringe maxima are symmetrical in angular position and reflectivity around the main diffraction maxima ($\omega=0$), i.e., the interference fringes of the order $+n$ and $-n$ are of the same intensity.

It is of special interest to investigate the x-ray interference phenomena (Pendellösung) in multilayers in order to achieve the structural parameters of the constituent thin and ultrathin single layers on the nanometer scale. The reflection amplitude Φ_n of a heterostructure composed of n layers is[22]

$$\Phi_n=i(|\gamma_0/\gamma_h|)^{1/2}\sum_{j=1}^{n}[a_j\exp(-i\phi_j)\Phi_j] , \tag{6}$$

where a_j is the factor taking into account absorption and ϕ_j contains the phase relations of the wave fields according to

$$\phi_j=A_jY_j+2\sum_{i=1}^{j-1}(A_iY_i) . \tag{7}$$

We consider now the reflectivity of a double heterostructure. Using Eqs. (6) and (7) we obtain for the reflectivity

$$R_2=\Phi_1^2+\Phi_2^2+2\Phi_1\Phi_2\cos(\phi_2-\phi_1) . \tag{8}$$

The x-ray reflectivity of a heterostructure composed of three layers, where a thin layer 0 is sandwiched between the layers 1 and 2 is given by

$$\begin{aligned}R_3=&\Phi_1^2+\Phi_2^2+\Phi_0^2\\&+2[\Phi_1\Phi_0\cos(\phi_0-\phi_1)+\Phi_2\Phi_1\cos(\phi_2-\phi_1)\\&+\Phi_2\Phi_0\cos(\phi_2-\phi_0)] .\end{aligned} \tag{9}$$

The difference between the diffraction patterns given by Eqs. (8) and (9) is due to the thin layer 0. We assume, for simplicity, that the layers 1 and 2 are of the same thickness $\Delta_1=\Delta_2=\Delta_c$ and have the same chemical composition, structure factor, and lattice constant. The difference in reflectivity is than given by

$$\begin{aligned}\Delta R&=R_3-R_1\\&=\Phi_0^2+2\Phi_c\Phi_0[\cos(A_cY_c+A_0Y_0)+\cos(2A_cY_c)]+2\Phi_c^2\{\cos[2(A_cY_c+A_0Y_0)]-\cos(2A_cY_c)\} .\end{aligned} \tag{10}$$

We are now most interested in the case where the thickness of the thin layer δ is much smaller than the thickness of the cladding layers Δ_c ($\delta\ll\Delta_c$) and consequently the scattering power of the thin layer is very small and $\Phi_0\ll\Phi_c$. Under these conditions the first and second terms in Eq. (10) can be neglected. Equation (10) can be simplified to the form

$$\Delta R\simeq 4\Phi_c^2[\sin(A_0Y_0+2A_cY_c)\sin(A_0Y_0)] . \tag{11}$$

The important result is that the difference in reflectivity caused by the sandwiched layer 0 is given by the reflectivity of the cladding layers which is modulated by

two sinusoidal functions describing the phase shift of the wave fields between the layers 1 and 2 separated by the thin layer 0. The first sinusoidal term depends on the total thickness of the heterostructure, while the second term is a function of the structural parameters of the thin sandwiched layer only. The argument of the second sinusoidal term is

$$A_0 Y_0 = -\pi \sin(2\theta_B)\delta(\omega+s)/(\lambda|\gamma_h|) , \quad (12)$$

where s is the strain function[2]

$$s = \epsilon_z[\cos^2(\alpha)\tan(\theta_B)+\tfrac{1}{2}\sin(2\alpha)] - \epsilon_x[\sin^2(\alpha)\tan(\theta_B)-\tfrac{1}{2}\sin(2\alpha)] , \quad (13)$$

where ϵ_z and ϵ_x are the lattice strain perpendicular and parallel to the crystal surface, respectively, and α is the angle between the crystal surface and the reflecting plane.

The phase shift between the wave fields is related to the product δs. We call the product of lattice strain and thickness of the sandwiched layer "phase-shift parameter" ($\Xi = \delta s$), since the wave fields of the layers 1 and 2 are decoupled due to the spatial separation of the layers. Equation (13) shows that the modulation of the reflectivity increases with increasing layer thickness and increasing strain.

In summary, we may conclude that the kinematical diffraction theory predicts an intensity modulation of the Pendellösung fringes caused by a phase shift of the waves which are scattered by different layer portions. The change in reflectivity due to a thin layer sandwiched between two cladding layers is a function of (i) the reflectivity of the cladding layers (i.e., their thickness), and (ii) the strain and the thickness of the sandwiched layer. However, the kinematical approximation does not take into account the interference between heterostructure and substrate. But for some cases, especially if the lattice strain between epilayer and substrate is small as it occurs in the $Al_xGa_{1-x}As/GaAs$ material system, this interference cannot be neglected.[23,24] For the simulation of the experimental diffraction patterns it is then necessary to use the dynamical diffraction theory, since only this theory allows us to take into account the interference of the wave fields between the whole epilayer structure and the thick substrate. The dynamical theory gives the exact boundary conditions at the heterointerfaces, which are needed to describe the true phase shift and absorption effect. Therefore, in our work the dynamical diffraction theory in the recursive formalism[4,5] is used to calculate the diffraction patterns.

IV. RESULTS AND DISCUSSION

A. Type-*A* heterostructure

The type-*A* layer structure is schematically shown in Fig. 1. A single GaAs layer of thickness δ is sandwiched between confining $Al_xGa_{1-x}As$ and $Al_yGa_{1-y}As$ layers of thickness Δ_1 and Δ_2 and composition x and y, respectively. The x-ray waves Φ_{h,Δ_1} and Φ_{h,Δ_2} scattered by the two (AlGa)As layers are decoupled due to the GaAs layer

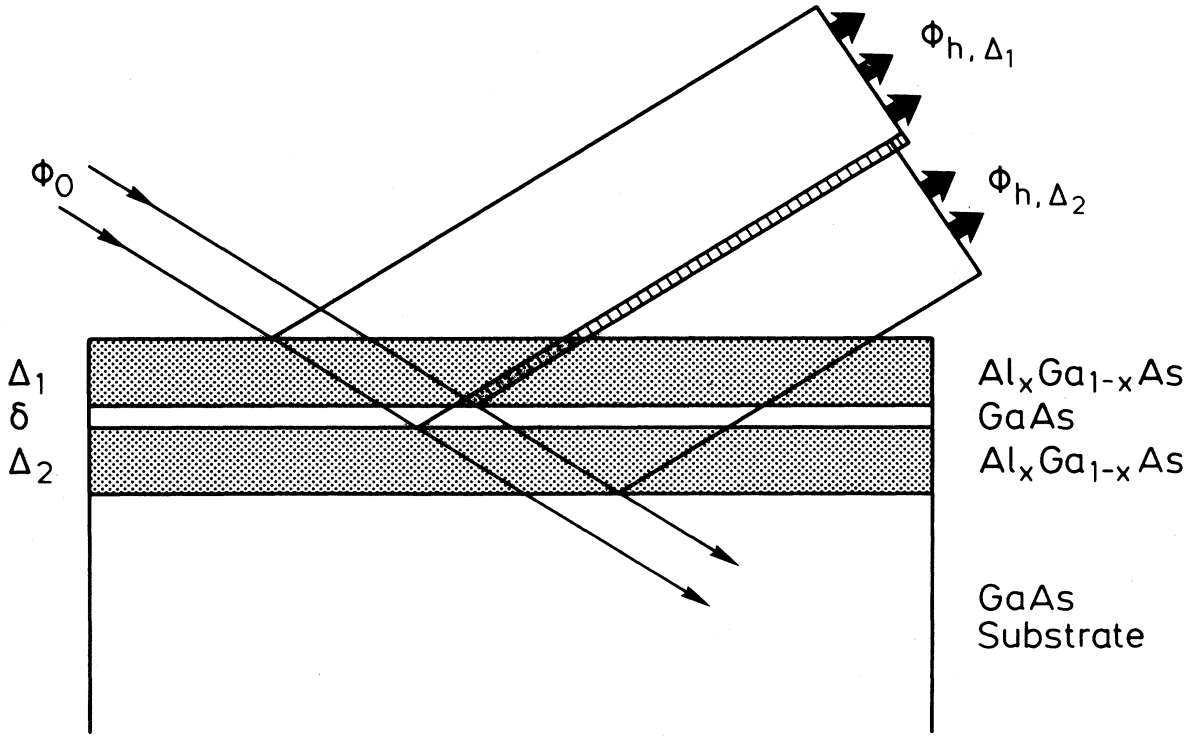

FIG. 1. Schematic diagram of the x-ray scattering and the interference of x-ray wave fields on an $Al_xGa_{1-x}As/GaAs$ heterostructure of type *A* (see text).

which spatially separates the two confining layers. The separation by the GaAs layer with a slightly different lattice parameter perpendicular to the crystal surface with respect to the (AlGa)As layers causes a phase shift between the scattered waves Φ_{h,Δ_1} and Φ_{h,Δ_2}. The diffracted waves of the two (AlGa)As layers interfere as shown in Fig. 1, and this produces a modulation of the amplitude of the interference fringes, which can be observed in the diffraction curve. Under real experimental conditions the size of the x-ray beam incident on the specimen will be much larger than the thickness of the epilayer structure ($\simeq 1$ μm) and therefore the area in which the two wave fields interfere is much broader than that shown in the scheme of Fig. 1. This means that the diffracted beam of the epilayer structure is mainly an interference between the two waves Φ_{h,Δ_1} and Φ_{h,Δ_2}.

Figure 2 shows the computed (400) diffraction curves of a layer structure with GaAs layer thicknesses of $\delta=0$ and 6 nm, respectively. The structural parameters of the $Al_xGa_{1-x}As$ layers are $\Delta_1=\Delta_2=350$ nm and the Al mole fraction $x=y=0.35$. The diffraction peaks of the two constituent materials are located at different angular positions due to the different lattice constants perpendicular to the crystal surface between the (AlGa)As layer and the GaAs substrate. The lattice spacing of the Al_xGa_{1-xs} is $a_0(1+2.82\times10^{-3}x)$, where a_0 is the lattice spacing of GaAs ($=0.282\,675$ nm).[2] Around the main epilayer peak (labeled by *E*), interference fringes appear. The angular distance $\Delta\omega_p$ between two fringe maxima is related to the total epilayer thickness $D_e=\Delta_1+\Delta_2+\delta$ by Eq. (4). The presence of a thin GaAs layer causes a phase shift between the waves diffracted by two (AlGa)As layers and this consequently produces a modulation of the amplitude of the interference fringes. Some interference maxima are increased in intensity, while others are decreased (Fig. 2). The modulation becomes more pronounced with increasing GaAs layer thickness δ as shown in Fig. 3. The dependence of the intensity modulation of the interference fringes by the layer thickness δ allows us to determine with high accuracy the thickness δ even of very thin layers in the nm scale.

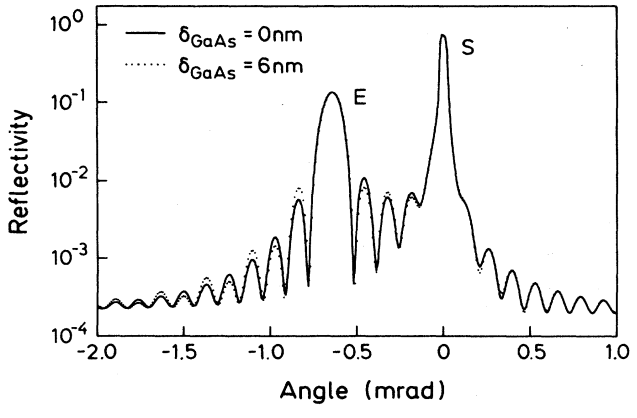

FIG. 2. Calculated (400) diffraction patterns (Cu $K\alpha_1$ radiation) for the heterostructure shown in Fig. 1. The thickness of the cladding layers is $\Delta_1=\Delta_2=350$ nm and their Al composition is $x=y=0.35$, while the GaAs quantum wells are 0 nm (solid line) and 6 nm (dotted line) thick.

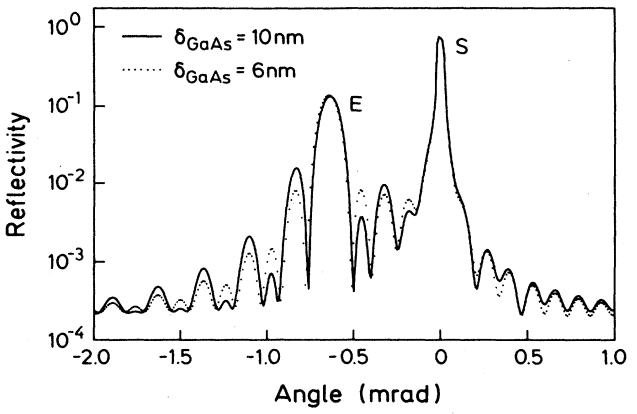

FIG. 3. Calculated x-ray diffraction patterns around the (400) GaAs reflection of heterostructures with similar structural parameters as in Fig. 2, but with increased GaAs quantum-well thickness.

The period of the intensity modulation depends on the ratio of the thicknesses of the confining (AlGa)As layers, i.e., Δ_1/Δ_2. Assuming $\Delta_2=n\Delta_1$ then we can observe in the diffraction spectra an increase (or decrease) of each $(n+1)$th interference maximum, where $n+1=(\Delta_1+\Delta_1)/\Delta_1$. For example, if $\Delta_1=\Delta_2$, each second interference maximum will be increased (or decreased) in reflectivity (Figs. 2 and 3). However, if n is not an integer, a shift of the interference maxima can be observed as shown in Fig. 4. The total thickness of the cladding layers is $\Delta_1+\Delta_2=700$ nm, while the Al mole fraction is $x=y=0.35$ as for the examples given in Figs. 2 and 3, and t_s is defined as $t_s=\Delta_s-\Delta_1$. Here, Eq. (4) is no longer valid and a comparison between the experimental and the computed diffraction curves is necessary to obtain the exact values of the thicknesses Δ_1, Δ_2, and δ and the Al

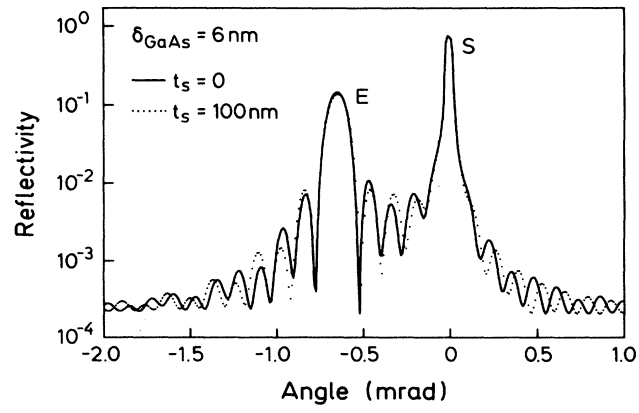

FIG. 4. Calculated (400) diffraction patterns of 6-nm-thick single quantum wells with symmetrical (solid line) and asymmetrical (dotted line) $Al_xGa_{1-x}As$ confinement layers (see text).

mole fractions x and y.

Figure 5 shows the experimental (dotted line) and the corresponding simulated (solid line) x-ray diffraction curve in the vicinity of the symmetrical (400) reflection. The angular fringe spacing is determined to be 43 μrad, which gives a total epilayer thickness $D_e = 2136(\pm 30)$ nm. The reflectivity modulation of the interference peaks is well pronounced and demonstrates clearly the existence of a thin GaAs layer in between the (AlGa)As epilayers. The simulation of the experimental diffraction curve gives the following parameters for the epilayer structure: $\Delta_1 = \Delta_2 = 1060(\pm 20)$ nm, $x = y = 0.40(\pm 0.01)$ (this corresponds to a strain perpendicular to the crystal surface of $\epsilon_z = 11.5 \times 10^{-4}$) and $\delta = 5(\pm 1)$ nm. These values are in good agreement with the parameters derived from the growth conditions.

For many applications it is also of great interest to investigate the reflectivity modulation of the interference fringes for cases where the sandwiched GaAs layer becomes thicker. Figure 6 shows the calculated (400) diffraction curves of an epilayer structure with $\Delta_1 = \Delta_2 = 1000$ nm and $x = y = 0.35$. The thickness δ of the GaAs layer is 0, 10, and 100 nm for the curves (a), (b) and (c), respectively. For the case with $\delta = 10$ nm [Fig. 6(b)] a well-pronounced reflectivity modulation of the interference maxima around the main epilayer peak (labeled by E) is observed and the angular spacing between the substrate peak S and the peak E is related to the strain in the epilayer structure. However, if the GaAs layer thickness is strongly increased [e.g., $\delta = 100$ nm for the curve in Fig. 6(c)] the main epilayer peak E is split and the angular distance between the maximum of the epilayer peak E and the GaAs peak S does not give the actual strain and chemical composition of the heterostructure. The reflectivity modulation of the interference peaks around the peak E is asymmetrical. In fact, between the epilayer peak E and the GaAs substrate peak S only the strong interference maxima are observed, while the damped interference maxima have disappeared. At the lower-angle wing of the epilayer peak E the typical features of the reflectivity modulation are observed. Similar diffraction curves from rather thick single layers sandwiched between two confinement layers have been observed and studied theoretically by Chu and Tanner.[25]

Finally, it should be noted that the reflectivity modulation of the interference fringes can be observed even if $\Delta_1 \neq \Delta_2$ and $x \neq y$. However, in this case the simulation of the experimental diffraction curves becomes more difficult.

B. Type-*B* heterostructure

The type-B layer structure is schematically shown in Fig. 7. Here a thin $Al_xGa_{1-x}As$ layer of thickness δ is

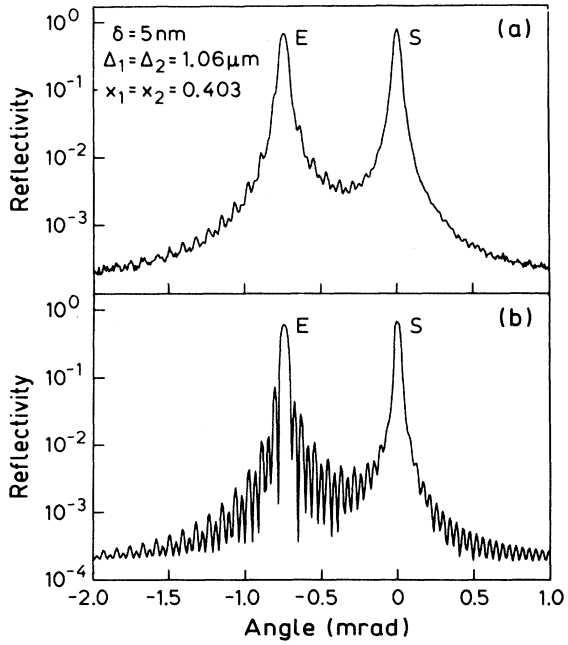

FIG. 5. (a) Experimental and (b) simulated (400) diffraction pattern of a 5-nm-thick GaAs single quantum well with symmetrical $Al_{0.403}Ga_{0.597}As$ (1.06 μm thick) cladding layers.

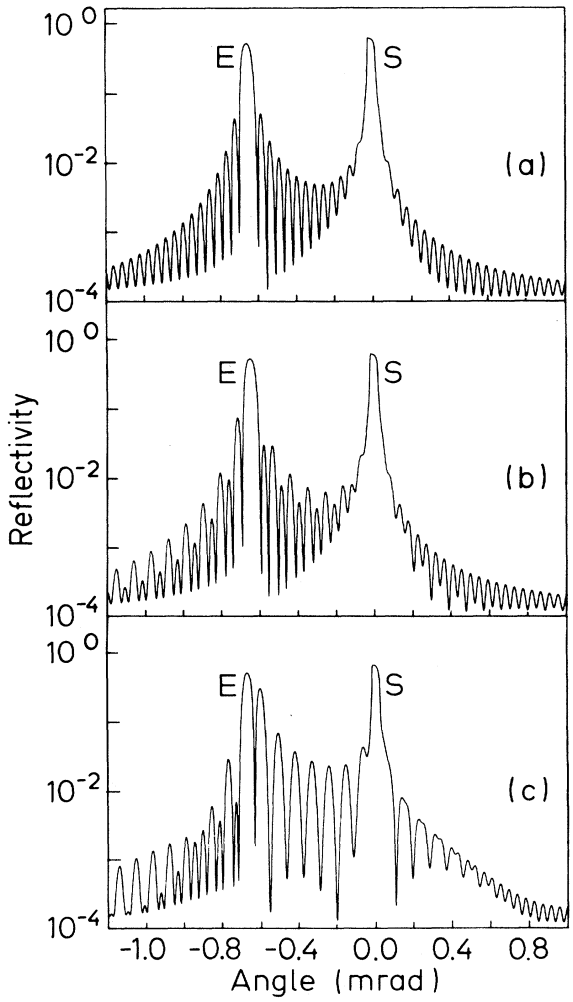

FIG. 6. Modulation of interference fringes around the (400) GaAs reflection of a double heterostructure as a function of the thickness δ of the active GaAs layer: (a) $\delta = 0$ nm, (b) $\delta = 10$ nm, and (c) $\delta = 100$ nm (see text).

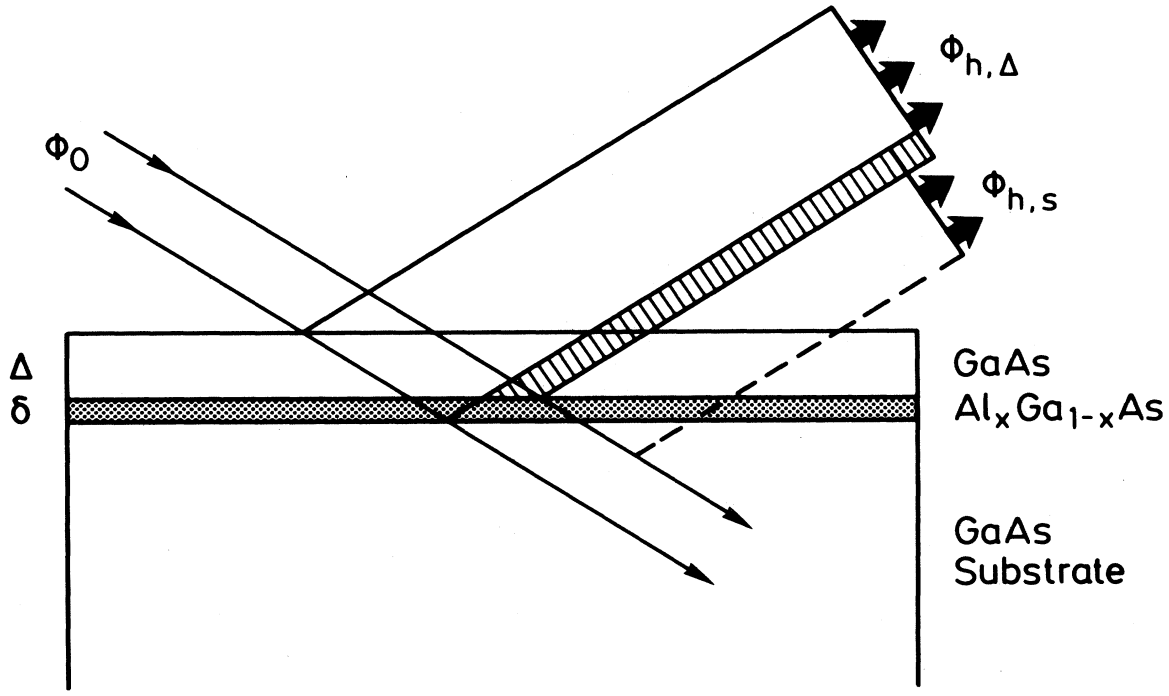

FIG. 7. Schematic diagram of the x-ray interference on a heterostructure consisting of the GaAs substrate, a thin $Al_xGa_{1-x}As$ layer, and a GaAs cap layer (structure of type *B*).

sandwiched between the GaAs substrate (and/or GaAs buffer layer) and a relatively thick GaAs cap layer of thickness Δ (~ 100 nm). As in the layer structure of type *A*, the GaAs substrate and the cap layer are spatially separated, and due to the lattice strain in the $Al_xGa_{1-x}As$, the lattice planes of the GaAs cap layer are not in phase with the lattice planes of the GaAs buffer layer (and/or GaAs substrate). Consequently, the wave $\Phi_{h,\Delta}$ diffracted from the GaAs cap layer is decoupled and phase shifted with respect to the wave $\Phi_{h,s}$ scattered from the buffer layer and/or the substrate crystal. The interference between the waves $\Phi_{h,\Delta}$ and $\Phi_{h,s}$ can be observed in the diffraction curve as an intensified Pendellösung effect.

A measure for the decoupling and phase shift between the waves $\Phi_{h,\Delta}$ and $\Phi_{h,S}$ is the product of the strain ϵ and thickness δ (phase shift parameter) of the sandwiched layer [see Eqs. (11) and (12)]. Figure 8 shows the (400) diffraction curves of a structure with the GaAs cap layer thickness of $\Delta = 500$ nm and for different $Al_{0.32}Ga_{0.68}As$ thicknesses δ. The phase shift parameter Ξ is 2.92, 5.84, and 11.7 nm mrad for the curves *A*, *B*, and *C*, respectively. The peak of the sandwiched $Al_xGa_{1-x}As$ layer (labeled by *E*) appears only as a shoulder of slightly increased reflectivity and is not separated from the GaAs substrate peak. It is therefore not possible to determine with accuracy the Al mole fraction by using the standard method,[2] which correlates the chemical composition and the angular distance between the $Al_xGa_{1-x}As$ and the GaAs peak (Vegard's rule). The interference fringes observed around the main GaAs peak (Fig. 8) are caused by the interference between the waves diffracted from the GaAs buffer layer (substrate) and the GaAs cap layer. The amplitudes of the fringes increase with increasing layer thickness δ, while the fringe spacing is related to the cap layer thickness Δ [Eq. (4)]. The relative position of the fringes with respect to the main GaAs peak is a function of the layer thickness δ and of the strain (chemical composition) within the heterostructure. Due to the boundary condition for the diffracted wave at the $Al_xGa_{1-x}As$/GaAs and GaAs/$Al_xGa_{1-x}As$ heterointerface the peak *E* ($Al_xGa_{1-x}As$ layer) shifts to higher

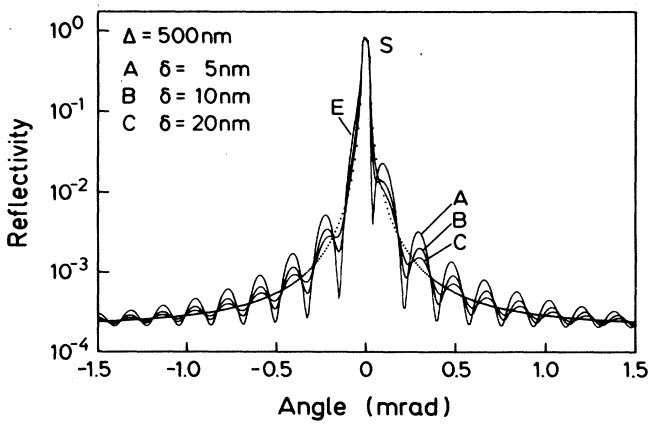

FIG. 8. Calculated x-ray diffraction patterns in the vicinity of the (400) GaAs reflection of a type-*B* structure for different thicknesses δ of the $Al_{0.32}Ga_{0.68}As$ layers.

angle.[24] This effect is clearly observed in Fig. 8, where it is manifested by the relative shift of the fringe maxima at higher diffraction angle. Thus, the angular position of the fringe maxima can be used to determine the mole fraction x of the $Al_xGa_{1-x}As$ layer. However, a computer simulation using the dynamical diffraction theory is needed.

The interference phenomena as a function of the thickness of the GaAs cap layer thickness Δ are studied and the results are depicted in Fig. 9. The diffraction curves are calculated in the vicinity of the symmetrical (400) GaAs cap layer thicknesses Δ (0, 100, and 200 nm), with constant $Al_xGa_{1-x}As$ layer thickness $\delta=10$ nm and the mole fraction $x=0.35$. It is evident that if the phase shift parameter becomes small ($\Xi<2$ nm mrad), the interference effect is rather weak and a thicker cap layer is needed to observe the fringes around the main peak.

The examples given in Figs. 8 and 9 indicate the sensitivity and accuracy of the x-ray Bragg diffraction to detect very thin epilayers and to determine their structural parameters, including layer thickness, lattice strain, and chemical composition. The method is not limited to symmetrical reflections only. Figure 10 shows the experimental (dotted line) and the corresponding computed diffraction curves (solid line) of the symmetrical (400) (a) and the asymmetrical (422) reflection (b) with ($|\gamma_h|>\gamma_0$). The simulation of the (400) and (422) experimental diffraction curves gives a thickness $\delta=22$ nm and the Al mole fraction $x=0.33$ ($\Xi=13.4$ nm mrad) for the $Al_xGa_{1-x}As$ layer, while the thickness of the GaAs cap layer is determined to be $\Delta=67$ nm.

Figure 11 shows the (a) experimental and (b) computed diffraction curves around the symmetrical (400) reflection of a heterostructure deposited on (100) GaAs substrate and composed of a GaAs buffer layer, a thin $Al_xGa_{1-x}As$ layer, and a GaAs cap layer. The layer thicknesses determined by the computer simulation are 112 nm for the GaAs cap layer and 25 nm for the (AlGa)As layer, while the Al mole fraction is $x=0.33$.

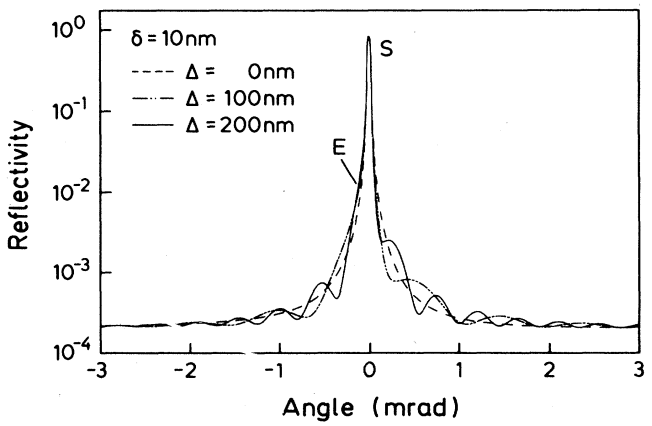

FIG. 9. Influence of the cap-layer thickness Δ on the (400) diffraction pattern. The Al mole fraction of the 10-nm-thick $Al_xGa_{1-x}As$ layer is kept constant for all three cases, i.e., $x=0.35$.

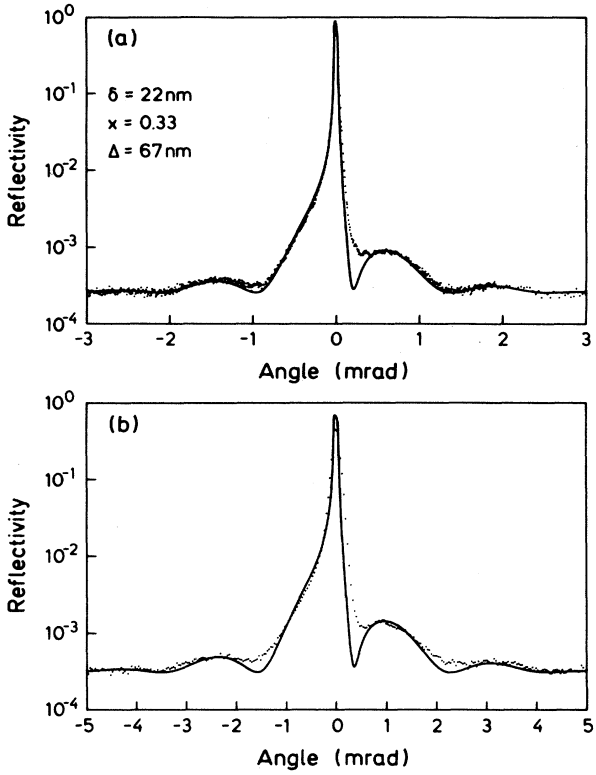

FIG. 10. Experimental (dotted lines) and simulated (solid lines) x-ray diffraction patterns of a type-*B* heterostructure in the vicinity of the (a) symmetrical (400) and the (b) asymmetrical (422) GaAs reflection.

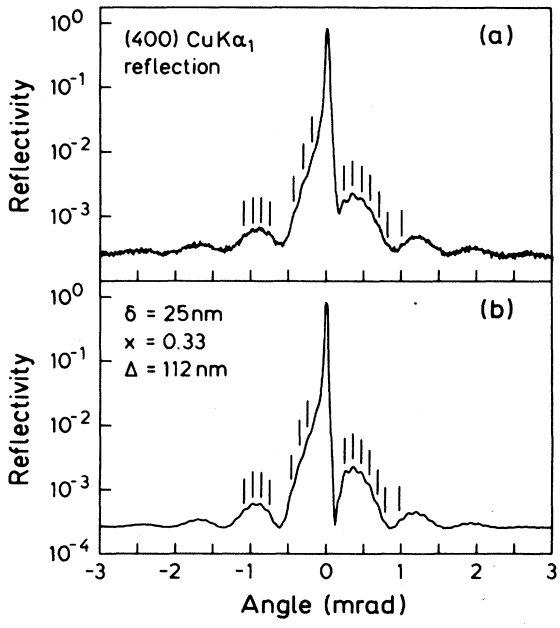

FIG. 11. (a) Experimental and (b) simulated (400) diffraction patterns of a type-*B* heterostructure. The short period interference fringes are caused by the interfacial strain between the GaAs substrate and the GaAs buffer layer. Some maxima of the short period fringes are marked by vertical lines.

Superimposed to the long-period interference fringes, caused by the phase shift between GaAs cap layer and GaAs substrate, is a short-period intensity oscillation, indicated by the vertical lines in Fig. 11. The appearance of these short-period intensity oscillations can be explained only if the lattice planes in the GaAs buffer layer are displaced with respect to the lattice planes in the GaAs substrate (phase shift). The best theoretical fit was obtained by assuming a strained interface between the GaAs substrate and the GaAs buffer layer with the transition thickness of 2 monolayers and a strain of 3×10^{-3} ($\Xi=1.1$ nm mrad). The angular distance between the short-period interference peaks is related to the thickness of the GaAs buffer layer, which is determined to be 750 nm and agrees very well with the value derived from the growth conditions. The thin and strained interface layer between the GaAs substrate and the GaAs buffer layer is probably caused by a contamination of the substrate surface before the epitaxial growth. In fact the surface of the substrate is intentionally covered with a thin oxide layer for passivation. This passivating oxide film on GaAs must be removed before the growth is initiated and this is easily done by heating the substrate crystal to the oxygen desorption temperature of 580 °C.[26] This process is usually controlled by observing the reflection high-energy electron diffraction (RHEED) pattern. Then, the substrate temperature is adjusted to the appropriate growth temperature (550–650 °C). It may sometimes happen that the oxide is not completely removed from the substrate surface and sometimes it may also be possible that the substrate surface is still slightly contaminated by other impurities. The impurity contamination of the substrate surface will cause a chemical reaction as the growth is initiated, thus forming a transition layer between the substrate crystal and the epilayer. The chemical nature of the transition layer is at present not known, but it is well established that the quality of the interface structure is of fundamental importance for the performance of optical and electronic devices. However, additional investigations like microprobe analysis and chemical lattice imaging[27] are required in order to know the microscopic and chemical structure of the transition layer.

C. HEMT heterostructure

The x-ray interference effect can be also used to study heterostructures having more complicated layer sequences. As the number of layers increases it will become more complicated to interpret the x-ray diffraction pattern and to find the structural parameters of the whole heterostructure. As an example we investigated a high-electron-mobility-transistor (HEMT) structure grown on a semi-insulating GaAs substrate. An AlAs/GaAs superlattice was used as a buffer layer in order to reduce the propagation of dislocations and defects originating from the substrate in the real device structure.[26,28] Figure 12 shows (a) the experimental and (b) calculated (400) diffraction patterns. Figure 13 shows the layer sequence of the structure together with the thicknesses and compositions of the individual layers as determined by the computer simulation. The best-fit parameters for thickness, strain, and composition of the individual layers are determined by minimizing the discrepancies between the experimental and calculated diffraction patterns using the trial-and-error method. The superlattice period and the thickness of the individual AlAs and GaAs layers are

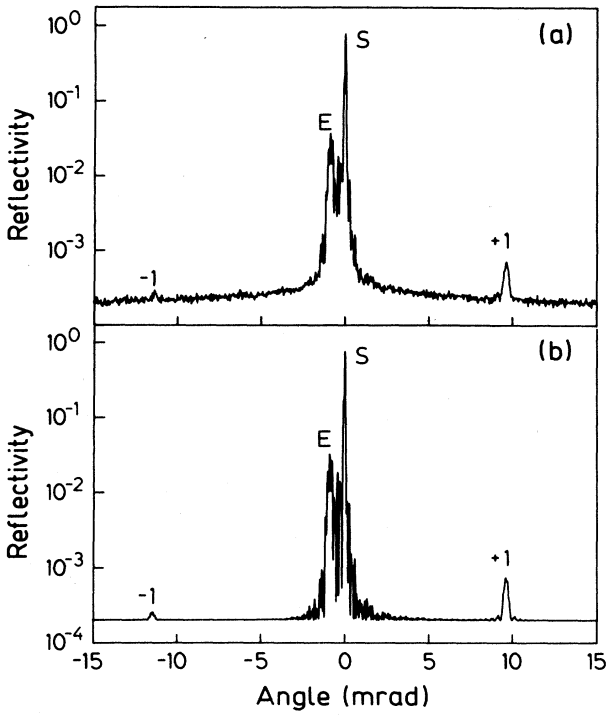

FIG. 12. (a) Experimental and (b) simulated (400) diffraction patterns of a HEMT structure. The appearance of the first-order satellite peaks is due to the AlAs/GaAs superlattice which is used as buffer layer.

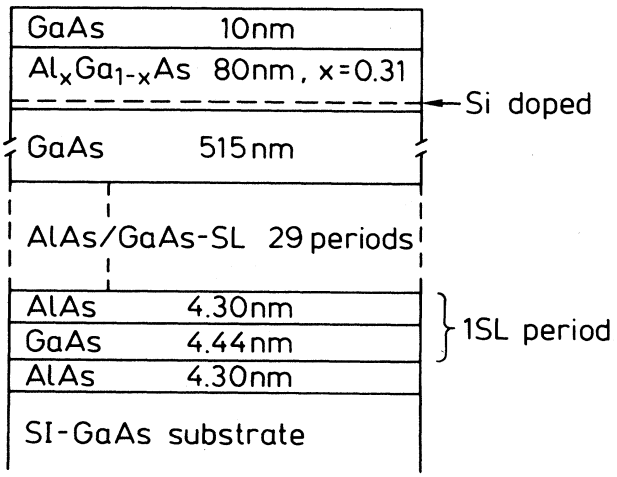

FIG. 13. Layer sequence of the HEMT structure together with the thicknesses and alloy compositions of the individual layers as determined by the computer simulation of the experimental diffraction pattern. (SI=semi-insulating, SL=superlattice)

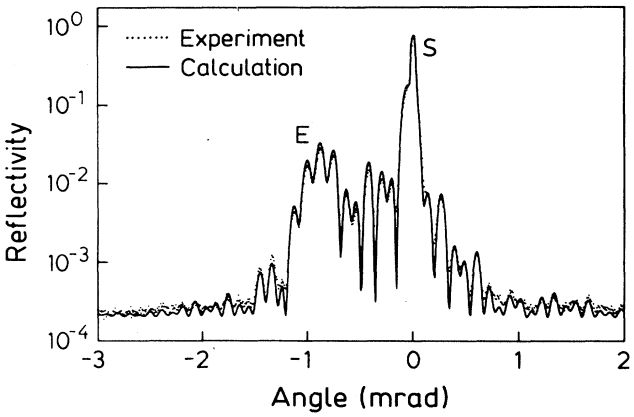

FIG. 14. Detail of the diffraction pattern shown in Fig. 12 very close to the (400) GaAs reflection on an enlarged scale. The angular position and the reflectivity modulation of the interference fringes include all information about the structural parameters of the whole heterostructure.

determined from their angular separation and their angular position (angular distance from the GaAs substrate peak labeled by *S*). To determine the structural parameters of the actual device structure it is necessary to investigate in detail the diffraction pattern very close to the GaAs substrate peak *S* shown in Fig. 14. Many strong interference peaks which are superimposed to a diffraction peak *E* attributed to the whole epilayer structure are observed. All the GaAs layer and the GaAs substrate scatter the incident x-ray beam at the same angular setting, but the wave fields undergo a phase shift due to the AlAs/GaAs superlattice and the $Al_xGa_{1-x}As$ layer, which separates the GaAs layers. Note that each constituent layer of the heterostructure is contributing to the shape of the whole diffraction pattern. Therefore, the intensities and positions of the interference peaks are an accurate measure of the structural parameters of the individual layers. The detailed structural analysis of HEMT heterostructures is of particular importance for the development of ultra-high-speed electron devices and integrated circuits.

V. CONCLUSION

X-ray interference fringes (Pendellösung) observed in the x-ray diffraction pattern are very sensitive to the presence of thin layers interspaced in heterostructures. The modulation in reflectivity and the angular position of the fringes provide detailed knowledge about the structural properties of thin epitaxial layers. The kinematical diffraction theory shows that the critical parameter for the reflectivity modulation is the product of lattice strain and thickness of the thin layer. A computer simulation of the experimental x-ray diffraction pattern using the dynamical theory allows one to determine the structural parameters like strain, thickness, and chemical composition of the whole heterostructure, even if the constituent layers are very thin (in the nanometer range). Additionally, the x-ray interference of wave fields scattered from different layers having a monolayer resolution can be used for the investigation of heterointerfaces (thickness of the transition region and of the interfacial strain).

ACKNOWLEDGMENTS

We wish to thank A. Fischer, H. Fronius, and M. Hauser for the sample preparation and R. Cingolani and F.-J. Stützler for critical reading of the manuscript. Part of this work was sponsored by the Bundesministerium für Forschung und Technologie (Bonn, Germany).

[1]V. S. Speriosu and T. Vreeland, Jr., J. Appl. Phys. **56**, 1591 (1984).
[2]L. Tapfer and K. Ploog, Phys. Rev. B **33**, 5565 (1986).
[3]M. A. G. Halliwell, M. H. Lyons, and M. J. Hill, J. Cryst. Growth **68**, 523 (1984).
[4]D. M. Vardanyan, H. M. Manoukyan, and H. M. Petrosyan, Acta Crystallogr. Sect. A **41**, 212 (1985).
[5]W. J. Bartels, J. Hornstra, and D. J. W. Loobek, Acta Crystallogr. Sect. A **42**, 539 (1986).
[6]U. Pietsch and W. Borchard, J. Appl. Crystallogr. **20**, 8 (1987).
[7]H.-G. Brühl, U. Pietsch, and B. Lengeler, J. Appl. Crystallogr. **21**, 240 (1988).
[8]C. A. Lucas, P. D. Hatton, S. Bates, T. W. Ryan, S. Miles, and B. K. Tanner, J. Appl. Phys. **63**, 1936 (1988).
[9]H. Rhan and U. Pietsch, Phys. Status Solidi A **107**, K93 (1988).
[10]T. Jach, P. L. Cowan, Q. Shen, and M. J. Bedzyk, Phys. Rev. B **39**, 5739 (1989).
[11]T. W. Ryan, P. D. Hatton, S. Bates, M. Watt, C. Sotomayor-Torres, P. A. Claxton, and J. S. Roberts, Semicond. Sci. Technol. **2**, 241 (1987).
[12]I. K. Robinson, Phys. Rev. B **33**, 3830 (1986).
[13]I. K. Robinson, R. T. Tung, and R. Feidenhans'l, Phys. Rev. B **38**, 3632 (1988).
[14]A. E. M. J. Fischer, E. Vlieg, J. F. van der Veen, M. Clausnitzer, and G. Materlik, Phys. Rev. B **36**, 4769 (1987).
[15]J. Zegenhagen, K.-G. Huang, B. D. Hunt, and L. J. Schowalter, Appl. Phys. Lett. **51**, 1176 (1987).
[16]Z. G. Pinsker, *Dynamical Scattering of X-Rays in Crystals* (Springer, Berlin, 1978).
[17]N. Kato and A. R. Lang, Acta Crystallogr. **12**, 787 (1959).
[18]B. W. Batterman and G. Hildebrandt, Acta. Crystallogr. Sect. A **24**, 150 (1968).
[19]B. K. Tanner and M. A. G. Halliwell, Semicond. Sci. Technol. **3**, 967 (1988).
[20]G. T. Baumbach, H. Rhan, and U. Pietsch, Phys. Status Solidi A **109**, K7 (1988).
[21]W. H. Zachariasen, *Theory of X-Ray Diffraction in Crystals* (Wiley, New York, 1945).
[22]V. S. Speriosu, J. Appl. Phys. **52**, 6094 (1981).
[23]P. F. Fewster and C. J. Curling, J. Appl. Phys. **62**, 4154 (1987).
[24]L. Tapfer, Phys. Scripta. **T25**, 45 (1989).
[25]X. Chu and B. K. Tanner, Appl. Phys. Lett. **49**, 1773 (1986).
[26]H. Fronius, A. Fischer, and K. Ploog, J. Cryst. Growth **81**, 169 (1987).
[27]A. Ourmazd, D. W. Taylor, J. Cunningham, and C. W. Tu, Phys. Rev. Lett. **62**, 993 (1989).
[28]M. Shinohara, Appl. Phys. Lett. **52**, 543 (1988).